

Selective Formic Acid Dehydrogenation Catalyzed by Fe-PNP Pincer Complexes Based on the 2,6-Diaminopyridine Scaffold

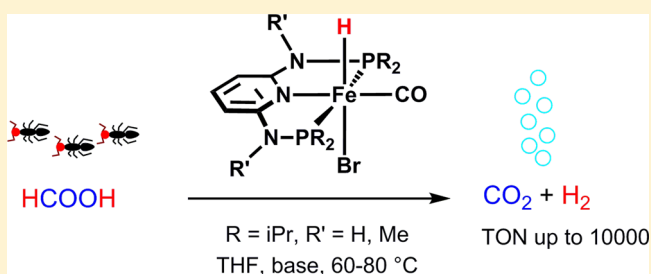
Irene Mellone,[†] Nikolaus Gorgas,[‡] Federica Bertini,[†] Maurizio Peruzzini,[†] Karl Kirchner,^{*,‡} and Luca Gonsalvi^{*,†}

[†]Consiglio Nazionale delle Ricerche (CNR), Istituto di Chimica dei Composti Organometallici (ICCOM), Via Madonna del Piano 10, 50019 Sesto Fiorentino (Firenze), Italy

[‡]Institute of Applied Synthetic Chemistry, Vienna University of Technology, Getreidemarkt 9/163-AC, A-1060 Wien, Austria

Supporting Information

ABSTRACT: Fe(II) hydrido carbonyl complexes supported by PNP pincer ligands based on the 2,6-diaminopyridine scaffold were studied as homogeneous, non-precious-metal-based catalysts for selective formic acid dehydrogenation to hydrogen and carbon dioxide, reaching quantitative yields and high TONs under mild reaction conditions.



INTRODUCTION

A global issue that scientists worldwide are called to answer is to provide solutions for sustainable energy production, by cleaner and renewable alternatives to fossil fuels. Hydrogen has been identified as an important energy vector, as its chemical bond energy can be converted into electricity using mature fuel cell technology.¹ Some of the major limitations to the widespread use of hydrogen for energy applications remain its efficient handling and storage, overcoming its safety issues, and improving its cost effectiveness.^{2,3} As a possible answer, a great deal of research has been carried out to identify suitable hydrogen-rich molecules from which hydrogen can be extracted reversibly under mild conditions of temperature and pressure.

Among several candidates,^{4–6} liquid organic hydrogen carriers (LOHCs),⁷ from which hydrogen can be released on demand by catalytic dehydrogenation, are receiving increasing attention. Among these, formic acid (FA), a liquid under ambient conditions having 4.4% in weight of hydrogen, can be safely handled, stored, and transported easily. Formic acid can be dehydrogenated under mild conditions in the presence of a suitable catalyst to afford fuel cell grade H₂ and CO₂ as the sole byproduct. In principle, CO₂ can be rehydrogenated to HCOOH, so a zero-carbon-emission energy storage cycle can be contemplated.⁸

In recent years, many different heterogeneous and homogeneous catalyst systems for the dehydrogenation of formic acid have been studied. In the case of homogeneous catalysts, the best results were obtained with noble-metal-based complexes, such as Ru⁹ and Ir.¹⁰ At present, an important target in organometallic catalysis is the replacement of noble-metal-based catalysts with non-precious-metal catalysts of comparable activity. Beller's group reported efficient hydrogen generation from formic acid catalyzed by either the in situ catalytic system

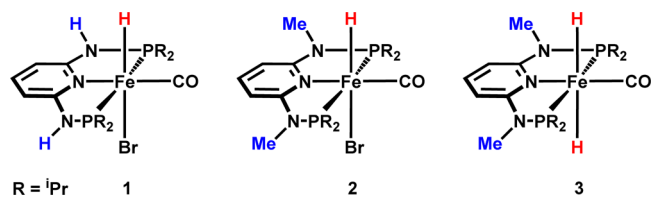
obtained from Fe(BF₄)₂·6H₂O and PP₃ ligand (PP₃ = tris[2-(diphenylphosphino)ethyl]phosphine) or the well-defined complexes [FeH(PP₃)]BF₄, [FeH(η²-H₂)(PP₃)]BF₄, [FeH(η²-H₂)(PP₃)]BPh₄, and [FeCl(PP₃)]BF₄ in propylene carbonate (PC) as solvent, without the need for an additional base. Except for [FeCl(PP₃)]BF₄, excellent activities were observed for all these systems, with a maximum TOF of 1942 h^{−1} after 3 h at 40 °C using Fe(BF₄)₂·6H₂O/PP₃. Remarkably, this system showed a good performance¹¹ in continuous hydrogen production at 80 °C with TON = 92000 and TOF = 9425 h^{−1}. Lately, some of us reported hydrogen generation from formic acid catalyzed by iron complexes bearing the linear tetraphosphine 1,1,4,7,10,10-hexaphenyl-1,4,7,10-tetraphosphadecane (tetraphos-1), under mild reaction conditions with good activities.¹² Laurency and co-workers described the first Fe-based catalyst for the formic acid dehydrogenation in aqueous solution, using Fe(II) salts together with the water-soluble meta-trisulfonated analogue of PP₃, namely PP₃TS.¹³ Recently, Milstein and co-workers described the iron dihydride pincer complex *trans*-[Fe-(tBuPNP)(H)₂(CO)] (tBuPNP = 2,6-bis(di-*tert*-butylphosphinomethyl)pyridine), which showed an outstanding activity and selectivity in formic acid dehydrogenation at 40 °C in the presence of trialkylamines, with TONs up to 100000.¹⁴ Finally, Schneider, Hazari, Bernskoetter and co-workers reported a new pincer-type iron catalyst that, without the need for added base or free ligand, in the presence of a Lewis acid (LA) as cocatalyst (10 mol %) at 60 °C, achieved the highest TON (ca. 1000000) reported for formic acid dehydrogenation using a first-row transition-metal catalyst.¹⁵

Received: July 8, 2016



In recent times, some of us synthesized new transition-metal complexes containing PNP pincer ligands based on the 2,6-diaminopyridine scaffold containing NH and NR linkers between the aromatic pyridine ring and the phosphine moieties.¹⁶ In particular, the iron complexes [Fe(PNP^H-iPr)(H)(CO)(Br)] (**1**) and [Fe(PNP^{Me}-iPr)(H)(CO)(Br)] (**2**) proved to be active catalysts for ketone and aldehyde hydrogenation.^{16c,h} Very recently we used complexes **1** and **2** (Chart 1) as catalysts for CO₂ and NaHCO₃ hydrogenation,

Chart 1. Fe-PNP Pincer Complexes 1–3



obtaining good results even under very mild conditions of temperature and pressure.¹⁷ A key role in catalysis was played by the in situ formed complex *trans*-[Fe(PNP^{Me}-iPr)-(H)₂(CO)] (**3**). Encouraged by these results, we decided to explore the possible application of these complexes as catalysts for formic acid dehydrogenation. Hereby we present a series of experimental results including detailed screening of reaction conditions and mechanistic considerations based on stoichiometric NMR reactions, which allowed for the description of a proposed catalytic cycle for these systems.

RESULTS AND DISCUSSION

Formic Acid Dehydrogenation Tests. We have tested complexes **1** and **2** for catalytic formic acid dehydrogenation under isobaric conditions at atmospheric pressure in the presence of added bases and additives and different solvents, temperatures, and catalyst loadings. The development of gases during the catalytic tests was measured with a manual gas buret. Aliquots of the gas mixtures produced were analyzed off-line by FT-IR, showing the absence of CO for all tests (see the Experimental Section).

Initially, we checked the activity of complexes **1** and **2** using formic acid without added base, but no activity was observed under these conditions, in contrast to the iron phosphine based systems reported in the literature.^{11,12,15}

We therefore applied the reaction conditions previously described by Milstein et al.¹⁴ for a similar pincer complex: i.e., adding 50 mol % of NEt₃ (0.5 equiv to FA) as base. To our delight, complexes **1** and **2** were found to be catalytically active under these reaction conditions. Using 0.1 mol % of the catalysts at 60 °C, formic acid dehydrogenation took place with TOF_{1h}s (turnover frequencies at 1 h) of 95 and 276 h^{−1} and TONs (turnover numbers) of 200 and 653 within 3 h in the case of **1** and **2**, respectively (Table 1, entries 1 and 2).

The presence of a base appeared to be mandatory for the reaction to occur. Initially, we tested the effect of different amounts of NEt₃ as base on the catalytic activity (Table 1). For complex **2**, lowering the amount of NEt₃ to 25 mol % led to a significant decrease in the catalytic activity (TON = 204, entry 3). On the other hand, better performances were obtained in

Table 1. Formic Acid Dehydrogenation using Fe-PNP complexes 1–3 Screening FA/Base Ratios, FA Concentrations, Nature of Base, Solvent, Temperature, and Catalyst Concentration Effects^a

| entry | catalyst | [FA] (mol/L) | solvent | base (mol %) | T (°C) | TOF _{1h} (h ^{−1}) ^c | TON ^d | conversn (%) |
|-----------------|----------|--------------|-------------|------------------------|--------|---|------------------|--------------|
| 1 | 1 | 2.5 | THF | NEt ₃ (50) | 60 | 95 | 200 (3) | 20 |
| 2 | 2 | 2.5 | THF | NEt ₃ (50) | 60 | 276 | 653 (3) | 65 |
| 3 | 2 | 2.5 | THF | NEt ₃ (25) | 60 | 102 | 204 (3) | 20 |
| 4 | 2 | 2.5 | THF | NEt ₃ (100) | 60 | 398 | 816 (3) | 82 |
| 5 | 2 | 2.5 | THF | NEt ₃ (200) | 60 | 418 | 827 (3) | 83 |
| 6 | 1 | 2.5 | THF | NEt ₃ (100) | 60 | 174 | 369 (3) | 37 |
| 7 | 2 | 5.0 | THF | NEt ₃ (100) | 60 | 612 | 1000 (2.5) | 100 |
| 8 | 2 | 10.0 | THF | NEt ₃ (100) | 60 | 770 | 1000 (2) | 100 |
| 9 | 1 | 5.0 | THF | NEt ₃ (100) | 60 | 716 | 1000 (2) | 100 |
| 10 | 2 | 5.0 | THF | NEt ₃ (50) | 60 | 593 | 980 (3) | 98 |
| 11 | 2 | 5.0 | THF | DMOA (50) | 60 | 673 | 980 (3) | 98 |
| 12 | 2 | 5.0 | THF | DBU (50) | 60 | 459 | 571 (3) | 57 |
| 13 | 1 | 5.0 | THF | DMOA (50) | 60 | 51 | 76 (3) | 2 |
| 14 | 2 | 5.0 | PC | NEt ₃ (100) | 60 | 500 | 1000 (3) | 100 |
| 15 | 2 | 5.0 | 1,4-dioxane | NEt ₃ (100) | 60 | 378 | 878 (3) | 88 |
| 16 | 2 | 5.0 | EtOH | NEt ₃ (100) | 60 | 165 | 650 (3) | 65 |
| 17 | 2 | 5.0 | THF | NEt ₃ (100) | 40 | 79 | 180 (3) | 18 |
| 18 | 2 | 5.0 | PC | NEt ₃ (100) | 60 | 500 | 1000 (3) | 100 |
| 19 ^e | 2 | 5.0 | PC | NEt ₃ (100) | 80 | 1800 | 1000 (0.6) | 100 |
| 20 ^b | 2 | 10.0 | THF | NEt ₃ (100) | 60 | 918 | 2245 (6) | 22 |
| 21 ^b | 2 | 10.0 | PC | NEt ₃ (100) | 80 | 2635 | 10000 (6) | 100 |
| 22 ^b | 2 | 5.0 | PC | NEt ₃ (100) | 80 | 1714 | 6286 (6) | 63 |
| 23 | 3 | 5.0 | THF | - | 60 | 0 | 0 (3) | 0 |
| 24 | 3 | 5.0 | THF | NEt ₃ (100) | 60 | 633 | 1000 (2) | 100 |

^aReaction conditions unless specified otherwise: 10.0 μmol of catalyst; 10.0 mmol of FA, specified amount of base, specified solvent. ^bReaction conditions: 5.0 μmol of catalyst; 50.0 mmol of FA, specified amount of base, specified solvent. Gas evolution was measured with a manual gas buret.

^cDefined as mmol_{H₂ produced}/(mmol_{catalyst} h), calculated after 1 h. ^dDefined as mmol_{H₂ produced}/mmol_{catalyst}. Run times (h) are given in parentheses.

^eTOF calculated after 20 min due to fast reaction. All tests were repeated at least twice to check for reproducibility (error ±10%).

the presence of 100 mol % (1 equiv to FA) of NEt_3 (TON = 816, entry 4). It is worth noting that under these conditions the activity shown by **2** was comparable to that of Milstein's catalyst.¹⁴ A further increase of amine content to 200 mol % did not lead to a significant improvement (TON = 827, entry 5). The catalytic activity of complex **1** also increased using 100 mol % of NEt_3 (entry 6 vs 1), although also under these conditions catalyst **1** performed less efficiently than **2** (TON = 369, entry 6).

Substrate concentration effects were then studied (Table 1, entries 4–9). For catalyst **2**, increasing the FA concentration from 2.5 to 10.0 mol/L resulted in an increase of $\text{TOF}_{1\text{h}}$ from 398 to 770 h^{-1} (entry 4 vs 8), and full conversions were achieved with FA concentrations of 5.0 and 10.0 mol/L (entries 7 and 8). Interestingly, catalyst **2** achieved complete conversion using a FA concentration of 5.0 mol/L, showing in this case a faster initial rate in comparison to **1** with a $\text{TOF}_{1\text{h}}$ of 716 h^{-1} (entry 9). A comparison of reaction profiles at various NEt_3 and FA concentrations is shown in Figure 1.

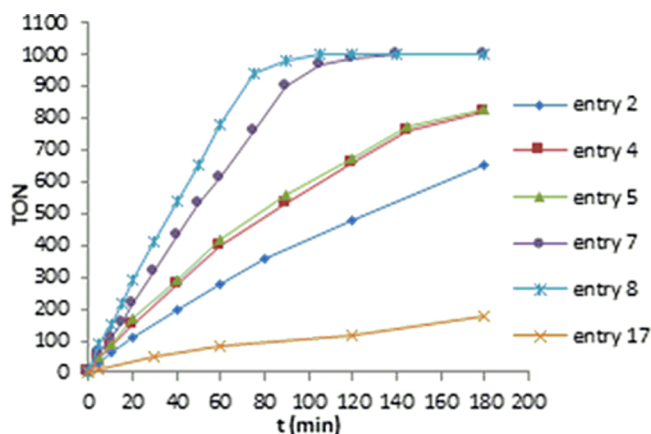


Figure 1. Reaction profiles of selected FA dehydrogenation tests run at 60 °C with **2** (0.1 mol %) with increasing amounts of NEt_3 (50 mol %, Table 1, entry 2; 100 mol %, entry 4; 200 mol %, entry 5), with increasing FA amounts (5.0 mol/L, entry 7; 10.0 mol/L, entry 8), and at a different temperature (40 °C, 5.0 mol/L FA, 100 mol % NEt_3 , entry 17). Other details are given in the footnotes of Table 1.

On the basis of these results, the effect of different amines and solvents on the catalytic activity was examined (Table 1, entries 10 to 12), showing that replacement of NEt_3 with other bases did not lead to any remarkable improvement.^{14,18} Using complex **2**, with 50 mol % of dimethyloctylamine (DMOA), the TON was unchanged in comparison to that with NEt_3 , although $\text{TOF}_{1\text{h}}$ slightly increased from 593 to 673 h^{-1} (entry 10 vs 11). With DBU as base, the catalytic performance dropped with a TON of 571 and $\text{TOF}_{1\text{h}}$ of 459 h^{-1} (entry 12). Complex **1** showed no activity with DBU and was almost inactive with DMOA (entry 13).

The results of solvent screening showed that the highest catalytic activity was achieved in aprotic solvents such as THF ($\text{TOF}_{1\text{h}}$ = 612 h^{-1} , Table 1, entry 7), propylene carbonate (PC, $\text{TOF}_{1\text{h}}$ = 500 h^{-1} , entry 14), and 1,4-dioxane ($\text{TOF}_{1\text{h}}$ = 378 h^{-1} , entry 15), whereas the use of a protic solvent such as EtOH resulted in significantly lower reaction rates ($\text{TOF}_{1\text{h}}$ = 165 h^{-1} , entry 16). The same order THF > PC > 1,4-dioxane > EtOH was observed for TONs and FA conversions at 3 h reaction time.

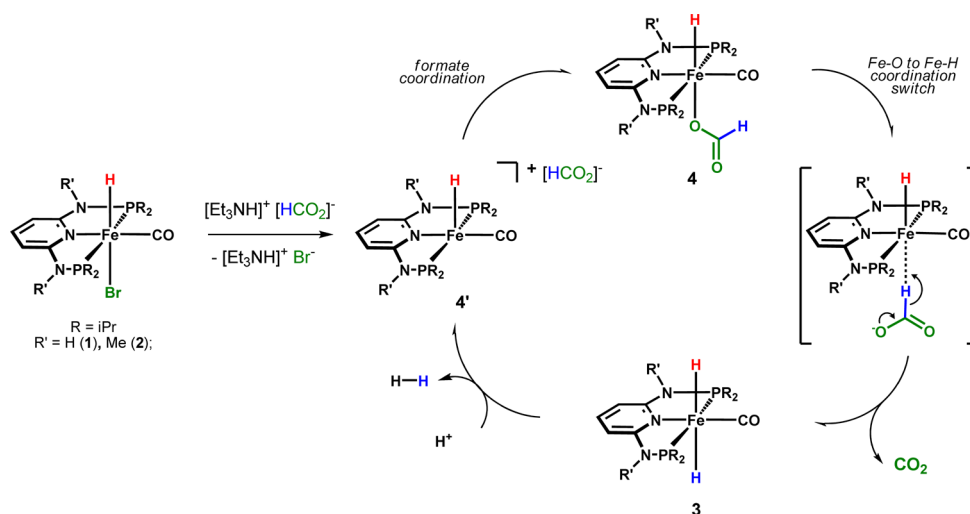
The effect of Lewis acids as cocatalysts was then tested. As recently reported by Hazari et al. for other Fe pincer based systems,¹⁵ such additives can accelerate FA dehydrogenation dramatically. However, this was not the case for our systems, as no FA conversion was observed under standard reaction conditions in the presence of LiBF_4 (10 mol %) instead of bases using complexes **1**–**3**.

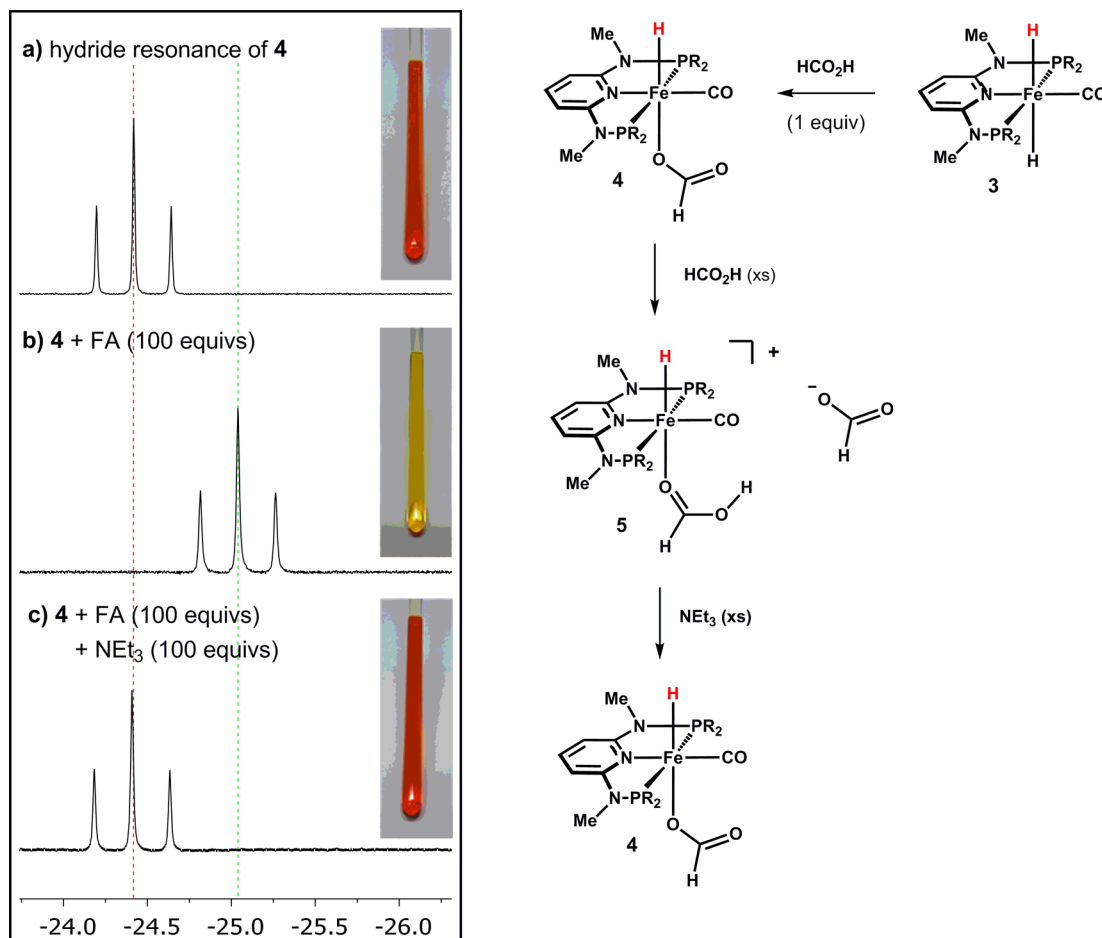
The effect of temperature was then evaluated for **2** (Table 1, entries 17–19). TON = 180 and $\text{TOF}_{1\text{h}}$ = 79 h^{-1} were obtained at 40 °C using a 2:FA ratio of 1:1000 (entry 17) after 3 h. To test higher temperature conditions, PC was used as a solvent. In this case, complete conversion (TON = 1000) was achieved at 80 °C after only 30 min, with a high $\text{TOF}_{1\text{h}}$ = 1000 h^{-1} (entry 19).

The effect of catalyst loading was studied in the case of reactions catalyzed by **2**.

When a catalyst to substrate ratio of 1:10000 was used at 60 °C with a FA concentration of 10.0 mol/L in THF, TON = 2245 was achieved after 6 h with a 22% conversion (Table 1, entry 20). When the test was run in PC at 80 °C, full conversion was reached within the same period, giving a rewarding TON of ca. 10000 (entry 21). Decreasing the FA

Scheme 1. Proposed Simplified Catalytic Cycle for FA Dehydrogenation Catalyzed by **1** and **2** (R = *i*Pr; R' = H, Me)



Scheme 2. Effect of Excess FA and Added Base on the Shift of the ^1H NMR Hydride Resonance of 4

concentration to 5.0 mol/L led to a significant decrease in the catalyst activity with a TON of 6286 and a conversion of 63% at 80 °C (entry 22).

Complex 3 was inactive in FA dehydrogenation in the absence of amine (entry 23), similarly to Milstein's catalyst,¹⁴ whereas it gave activity comparable to that of 1 and 2 in the presence of NEt_3 under the same test conditions (Table 1, entry 24 vs 7 and 9).

Then, a series of experiments with 2 were carried out to test catalyst deactivation vs product inhibition, by adding neat HCOOH aliquots (0.47 mL each) after the first run had reached 50% substrate conversion (see the Experimental Section). Using this procedure, an overall TON = 12170 was reached after ca. 8.5 h with an initial catalyst to substrate ratio of 1:5000 on running the test in PC at 80 °C. A decrease in activity was observed after the fourth addition. At an initial catalyst to substrate ratio of 1:1000, a higher number of consecutive cycles (11) was possible, reaching however a lower overall TON = 5574 after 4.5 h (see Table S7 and Figure S7 in the Supporting Information). Complex 3 (1:5000 catalyst to substrate ratio) gave results comparable to those for 2 under otherwise identical conditions (overall TON = 12300 after ca. 9 h).

Mechanistic Studies. A plausible mechanism for the catalytic dehydrogenation of formic acid with our complexes is outlined in Scheme 1. On the basis of our recent studies¹⁷ related to carbon dioxide hydrogenation, i.e. the reverse reaction of FA dehydrogenation, using catalysts 1 and 2, we

envisage that the latter proceeds via a very similar but reverse reaction pathway. The precatalysts (1 and 2) are activated by bromide abstraction, giving the coordinatively unsaturated cationic intermediate $[\text{Fe}(\text{PNP}-i\text{Pr})(\text{H})(\text{CO})]^+$ (4'). Subsequently, the formate ion may coordinate the iron metal center on the vacant site via the O atom, resulting in neutral $[\text{Fe}(\text{PNP}^{\text{Me}}-i\text{Pr})(\text{H})(\text{CO})(\eta^1\text{-OCOH})]$ (4). Then, the formate ligand switches from $\eta^1\text{-O}$ to $\eta^1\text{-H}$ coordination to Fe. Facile carbon dioxide elimination occurs, yielding 3, which upon hydride protonation releases H_2 to give back 4'.

To understand the role of the base in the mechanism, we performed a series of stoichiometric NMR experiments on the reactivity of precatalyst 2 with FA. No reaction could be observed after the addition of 10 equiv of neat FA to a solution of 2 in THF (with 20% C_6D_6 for deuterium lock), even upon heating the NMR tube to 60 °C for 1 h. On the other hand, when the experiment was repeated adding also 10 equiv of NEt_3 under otherwise identical conditions, the spectra revealed partial formation of complex 4 (ca. 25% on the basis of integration) and conversion of the substrate, as demonstrated by a decrease in the signals due to free formate. These observations confirm that a base is needed to activate the precatalyst, facilitating bromide dissociation and freeing a coordination site on the metal center.

It was observed experimentally (see above) that another role of amine is to promote catalytic turnover. This was confirmed by NMR experiments showing that addition of FA (1 equiv) to a solution of 3 in THF/ C_6D_6 (20%) caused immediate

formation of **4**, as demonstrated by the disappearance of the ^1H NMR triplet at -8.76 ppm ($J_{\text{PH}} = 42.9$ Hz) due to **3** and the appearance of a new triplet due to **4** at -24.4 ppm. Under these conditions, **4** proved to be stable in solution without evolving further. In a separate NMR experiment, addition of a known excess of FA (100 equiv) led to a slight shift of the hydride resonance of **4** in the ^1H NMR spectrum (-25.1 ppm), along with a significant color change of the respective solution from orange to bright yellow (Scheme 2). When NEt_3 (1 equiv to FA) was placed in the NMR tube, the hydride resonance shifted back to its initial value and also the color of the reaction solution turned back to orange.

We attribute this upfield shift of the hydride resonance to the change from an anionic (formate) to a neutral (FA) oxygen ligand coordinated trans to it. An excess of FA might thus lead to substitution/reprotonation of the formate ligand, resulting in the cationic complex $[\text{Fe}(\text{PNP}^{\text{Me}}\text{-iPr})(\text{H})(\text{CO})(\eta^1\text{-HCOOH})](\text{HCO}_2)$ (**5**), which in turn gives back **4** in the presence of added base.

The trend of the hydride resonances to shift toward more negative values is known for similar systems.^{16c,h,19} In our case, DFT calculations confirmed the chemical shift trend (see Scheme S1 in the Supporting Information). Thus, the role of the base in this step is to deprotonate the formic acid ligand in **5** to give back **4**, which in turn eliminates CO_2 and regenerates **3** by β -hydride elimination, closing the catalytic cycle.

CONCLUSIONS

In summary, we have shown that $\text{Fe}(\text{PNP})$ pincer-type complexes bearing the easily accessible and tunable 2,6-diaminopyridine scaffold are efficient catalysts for selective formic acid dehydrogenation, in the presence of added base, under mild reaction conditions. Studies are in progress to fine-tune the structure of the complexes in order to obtain more robust catalysts, allowing for improved long-term stability and more efficient recycling.

EXPERIMENTAL SECTION

General Methods and Materials. Complexes **1–3** were prepared according to recently reported procedures.^{16c} Formic acid, triethylamine, dimethyloctylamine, and DBU were purchased from commercial suppliers and degassed under nitrogen prior to use. All manipulations were carried out using standard Schlenk and glovebox techniques. Solvents were freshly distilled over appropriate drying agents, collected over Linde type 3 or 4 Å molecular sieves under nitrogen, and degassed with nitrogen or argon gas. Deuterated solvents for NMR measurements were purchased from commercial suppliers and stored onto activated 4 Å molecular sieves under Ar before use. The ^1H , $^{13}\text{C}\{^1\text{H}\}$, and $^{31}\text{P}\{^1\text{H}\}$ NMR spectra were recorded on a Bruker AVANCE-250 spectrometer (operating at 250.13, 101.26, and 62.90 MHz, respectively), on a Bruker Avance II 300 spectrometer (operating at 300.13, 75.47, and 121.50 MHz, respectively), and on a Bruker Avance II 400 spectrometer (operating at 400.13, 100.61, and 161.98 MHz, respectively) at room temperature. Peak positions are relative to tetramethylsilane and were calibrated against the residual solvent resonance (^1H) or the deuterated solvent multiplet (^{13}C). $^{31}\text{P}\{^1\text{H}\}$ NMR spectra were referenced to 85% H_3PO_4 with downfield shifts taken as positive.

Typical Procedure for FA Dehydrogenation Tests. In a typical experiment, a solution of catalyst (typically 0.010 mmol) in THF (2.0 mL) was placed under a nitrogen atmosphere in a magnetically stirred glass reaction vessel thermostated by external liquid circulation and connected to a reflux condenser and gas buret (2 mL scale). After the solution was heated to the desired temperature, NEt_3 (1.38 mL, 0.01 mol) and FA (0.38 mL, 0.01 mol) were added and the experiment was

started. The gas evolution was monitored throughout the experiment by reading the values of liquid displacement reached on the burets. The gas mixtures were analyzed off-line by FTIR spectroscopy using a 10 cm gas cell (KBr windows) to check for CO formation (detection limit 0.02%).²⁰ Each test was repeated at least twice for reproducibility.

Typical Procedure for Slow Substrate Feed Experiments. In a typical experiment carried out with the experimental setup described above, using either **2** or **3** (0.005 mmol), FA (initial amount 50 mmol), and NEt_3 (50 mmol) at a set temperature of 80 °C in PC as solvent, once 50% of the initial amount of FA had converted, neat FA (0.47 mL, 12.5 mmol) was added by syringe to the reaction vessel. The procedure was repeated until no further gas evolution was observed.

ASSOCIATED CONTENT

Supporting Information

The Supporting Information is available free of charge on the ACS Publications website at DOI: 10.1021/acs.organomet.6b00551.

Additional tables for catalytic tests for screening of various effects and corresponding reaction profiles and computational details for **4'** and **5** (PDF)

Cartesian coordinates for the calculated structure of **4'** (XYZ)

Cartesian coordinates for the calculated structure of **5** (XYZ)

AUTHOR INFORMATION

Corresponding Authors

*E-mail for K.K.: karl.kirchner@tuwien.ac.at.

*E-mail for L.G.: lgonsalvi@iccom.cnr.it.

Author Contributions

All authors have given approval to the final version of the manuscript.

Notes

The authors declare no competing financial interest.

ACKNOWLEDGMENTS

Financial contributions by the ECRF through projects HYDROLAB-2.0 and ENERGYLAB are gratefully acknowledged. This work was also supported by COST Action CM1205 CARISMA (Catalytic Routines for Small Molecule Activation) through an STSM for N.G. to the CNR. N.G. and K.K. gratefully acknowledge financial support by the Austrian Science Fund (FWF) (Project No. P28866–N34).

REFERENCES

- (1) (a) *Hydrogen as a future energy carrier*; Züttel, A., Boggschulte, A., Schlapbach, L., Eds.; Wiley: Hoboken, NJ, 2011. (b) Mazloomi, K.; Gomes, C. *Renewable Sustainable Energy Rev.* **2012**, *16*, 3024–3033. (c) Turner, J. A. *Science* **2004**, *305*, 972–974.
- (2) Crabtree, G. W.; Dresselhaus, M. S.; Buchanan, M. V. *Phys. Today* **2004**, *57*, 39–44.
- (3) (a) Schlapbach, L.; Züttel, A. *Nature* **2001**, *414*, 353–358. (b) Eberle, U.; Felderhoff, M.; Schüth, F. *Angew. Chem.* **2009**, *121*, 6732–6757.
- (4) (a) Darkrim, F. L.; Malbrunot, P.; Tartaglia, G. P. *Int. J. Hydrogen Energy* **2002**, *27*, 193–202. (b) Ströbel, R.; Garcke, J.; Moseley, P. T.; Jörissen; Wolf, L. G. *J. Power Sources* **2006**, *159*, 781–801.
- (5) (a) Sakintuna, B.; Lamari-Darkrim, F.; Hirscher, M. *Int. J. Hydrogen Energy* **2007**, *32*, 1121–1140. (b) Ley, M. B.; Jepsen, B.; Lars, H.; Young-Su, L.; Young-Whan, C.; von Colbe, B.; Dornheim, J. M.; Rokni, M.; Jensen, M.; Sloth, J. O.; Filinchuk, M.; Jorgensen, Y.

- Besenbacher, J. E.; Jensen, F.; Torben, R. *Mater. Today* **2014**, *17*, 122–128.
- (6) Langmi, H. W.; Ren, J.; North, B.; Mathe, M. K.; Bessarabov, D. *Electrochim. Acta* **2014**, *128*, 368–392.
- (7) (a) Okada, Y.; Sasaki, E.; Watanabe, E.; Hyodo, S.; Nishijima, H. *Int. J. Hydrogen Energy* **2006**, *31*, 1348–1356. (b) Wang, Z.; Tonks, I.; Belli, J.; Jensen, C. M. *J. Organomet. Chem.* **2009**, *694*, 2854–2857. (c) Wang, J.; Zhang, X. B.; Wang, Z.-L.; Wang, L.-M.; Zhang, Y. *Energy Environ. Sci.* **2012**, *5*, 6885–6888. (d) Johnson, T. C.; Morris, D. J.; Wills, M. *Chem. Soc. Rev.* **2010**, *39*, 81–88. (e) Alsabeh, P. G.; Mellmann, D.; Junge, H.; Beller, M. *Top. Organomet. Chem.* **2014**, *48*, 45–80. (f) Nielsen, M.; Alberico, E.; Baumann, W.; Drexler, H.-J.; Junge, H.; Gladiali, S.; Beller, M. *Nature* **2013**, *495*, 85–89. (g) Zeng, G.; Sakaki, S.; Fujita, K. I.; Sano, H.; Yamaguchi, R. *ACS Catal.* **2014**, *4*, 1010–1020. (h) Polukeev, A. V.; Petrovskii, P. V.; Peregudov, A. S.; Ezernitskaya, M. G.; Koridze, A. A. *Organometallics* **2013**, *32*, 1000–1015. (i) Kawahara, R.; Fujita, K. I.; Yamaguchi, R. *J. Am. Chem. Soc.* **2012**, *134*, 3643–3646. (j) Spasyuk, D.; Smith, S.; Gusev, D. G. *Angew. Chem., Int. Ed.* **2012**, *51*, 2772–2775. (l) Putignano, E.; Bossi, G.; Rigo, P.; Baratta, W. *Organometallics* **2012**, *31*, 1133–1142. (m) Bertoli, M.; Choualeb, A.; Lough, A. J.; Moore, B.; Spasyuk, D.; Gusev, D. G. *Organometallics* **2011**, *30*, 3479–3482. (n) Baratta, W.; Boss, G.; Putignano, E.; Rigo, P. *Chem. - Eur. J.* **2011**, *17*, 3474–3481. (o) Alberico, E.; Sponholz, P.; Cordes, C.; Nielsen, M.; Drexler, H. J.; Baumann, W.; Junge, H.; Beller, M. *Angew. Chem., Int. Ed.* **2013**, *52*, 14162–14166.
- (8) (a) Joó, F. *ChemSusChem* **2008**, *1*, 805–808. (b) Enthaler, S.; von Langermann, J.; Schmidt, T. *Energy Environ. Sci.* **2010**, *3*, 1207–1217. (c) Loges, B.; Boddien, A.; Gärtner, F.; Junge, H.; Beller, M. *Top. Catal.* **2010**, *53*, 902–914.
- (9) (a) Gao, Y.; Kuncheria, J.; Puddephatt, R. J.; Yap, G. P. A. *Chem. Commun.* **1998**, 2365–2366. (b) Fellay, C.; Dyson, P. J.; Laurenczy, G. *Angew. Chem., Int. Ed.* **2008**, *47*, 3966–3968. (c) Loges, B.; Boddien, A.; Junge, H.; Beller, M. *Angew. Chem., Int. Ed.* **2008**, *47*, 3962–3965. (d) Boddien, A.; Loges, B.; Junge, H.; Beller, M. *ChemSusChem* **2008**, *1*, 751–758. (e) Majewski, A.; Morris, D. J.; Kendall, K.; Wills, M. *ChemSusChem* **2010**, *3*, 431–434. (f) Boddien, A.; Loges, B.; Junge, H.; Gärtner, F.; Noyes, J. R.; Beller, M. *Adv. Synth. Catal.* **2009**, *351*, 2517–2520. (g) Li, X.; Ma, X.; Shi, F.; Deng, Y. *ChemSusChem* **2010**, *3*, 71–74. (h) Boddien, A.; Gärtner, F.; Federsel, C.; Sponholz, P.; Mellmann, D.; Jackstell, R.; Junge, H.; Beller, M. *Angew. Chem., Int. Ed.* **2011**, *50*, 6411–6414. (i) Boddien, A.; Federsel, C.; Sponholz, P.; Mellmann, D.; Jackstell, R.; Junge, H.; Laurenczy, G.; Beller, M. *Energy Environ. Sci.* **2012**, *5*, 8907–8911. (j) Rodríguez-Lugo, R. E.; Trincado, M.; Vogt, M.; Tewes, F.; Santiso-Quinones, G.; Grützmacher, H. *Nat. Chem.* **2013**, *5*, 342–347. (k) Mellone, I.; Peruzzini, M.; Rosi, L.; Mellmann, D.; Junge, H.; Beller, M.; Gonsalvi, L. *Dalton Trans.* **2013**, *42*, 2495–2501. (l) Sponholz, P.; Mellmann, D.; Junge, H.; Beller, M. *ChemSusChem* **2013**, *6*, 1172–1176. (m) Czaun, M.; Goeppert, A.; Kothandaraman, J.; May, R. B.; Haiges, R. G.; Prakash, K. S.; Olah, G. A. *ACS Catal.* **2014**, *4*, 311–320. (n) Filonenko, G. A.; Putten, R. V.; Schulpen, E. N.; Hensen, M. E. J.; Pidko, E. A. *ChemCatChem* **2014**, *6*, 1526–1530. (o) Pan, Y.; Pan, C.-L.; Zhang, Y.; Li, H.; Min, S.; Guo, X.; Zheng, B.; Chen, H.; Anders, A.; Lai, Z.; Zheng, J.; Huang, K.-W. *Chem. - Asian J.* **2016**, *11*, 1357–1360.
- (10) (a) Himeda, Y. *Green Chem.* **2009**, *11*, 2018–2022. (b) Tanaka, R.; Yamashita, M.; Chung, L. W.; Morokuma, K.; Nozaki, K. *Organometallics* **2011**, *30*, 6742–6750. (c) Hull, J. F.; Himeda, Y.; Wang, W. H.; Hashiguchi, B.; Periana, R.; Szalda, D. J.; Muckerman, J. T.; Fujita, E. *Nat. Chem.* **2012**, *4*, 383–388. (d) Maenaka, Y.; Suenobu, T.; Fukuzumi, S. *Energy Environ. Sci.* **2012**, *5*, 7360–7367. (e) Barnard, J. H.; Wang, C.; Berry, N. G.; Xiao, C. *Chem. Sci.* **2013**, *4*, 1234–1244. (f) Fukuzumi, S.; Kobayashi, T.; Suenobu, T. *J. Am. Chem. Soc.* **2010**, *132*, 1496–1497. (g) Oldenhof, S.; de Bruin, B.; Lutz, M.; Siegler, M. A.; Patureau, F. W.; van der Vlugt, J. I.; Reek, J. N. H. *Chem. - Eur. J.* **2013**, *19*, 11507–11511. (h) Suna, Y.; Ertem, M. Z.; Wang, W. H.; Kambayashi, H.; Manaka, Y.; Muckerman, J. T.; Fujita, E.; Himeda, Y. *Organometallics* **2014**, *33*, 6519–6530. (i) Wang, W. H.; Xu, S.; Manaka, Y.; Suna, Y.; Kambayashi, H.; Muckerman, J. T.; Fujita, E.; Himeda, Y. *ChemSusChem* **2014**, *7*, 1976–1983. (j) Wang, Z.; Lu, S.-M.; Li, J.; Wang, J.; Li, C. *Chem. - Eur. J.* **2015**, *21*, 12592–12595. (k) Papp, G.; Olveti, G.; Horváth, H.; Kathó, Á.; Joó, F. *Dalton Trans.* **2016**, DOI: 10.1039/C6DT01695B. (l) Celaje, J. J. A.; Lu, Z.; Kedzie, E. A.; Terrile, N. J.; Lo, J. N.; Williams, T. J. *Nat. Commun.* **2016**, *7*, 11308.
- (11) Boddien, A.; Mellmann, D.; Gaertner, F.; Jackstell, R.; Junge, H.; Dyson, P. J.; Laurenczy, G.; Ludwig, R.; Beller, M. *Science* **2011**, *333*, 1733–1736.
- (12) Bertini, F.; Mellone, I.; Ienco, A.; Peruzzini, M.; Gonsalvi, L. *ACS Catal.* **2015**, *5*, 1254–1265.
- (13) Montandon-Clerc, M.; Dalebrook, A. F.; Laurenczy, G. *J. Catal.* **2015**, DOI: 10.1016/j.jcat.2015.11.012.
- (14) Zell, T.; Butschke, B.; Ben-David, Y.; Milstein, D. *Chem. - Eur. J.* **2013**, *19*, 8068–8072.
- (15) Bielinski, E. A.; Lagaditis, P. O.; Zhang, Y.; Mercado, B. Q.; Würtele, C.; Bernskoetter, W. H.; Hazari, N.; Schneider, S. *J. Am. Chem. Soc.* **2014**, *136*, 10234–10237.
- (16) (a) Bichler, B.; Glatz, M.; Stöger, B.; Mereiter, K.; Veiros, L. F.; Kirchner, K. *Dalton Trans.* **2014**, *43*, 14517–15419. (b) de Aguiar, S. R. M. M.; Öztöpcü, Ö.; Stöger, B.; Mereiter, K.; Veiros, L. F.; Pittenauer, E.; Allmaier, G.; Kirchner, K. *Dalton Trans.* **2014**, *43*, 14669–14679. (c) Gorgas, N.; Stöger, B.; Veiros, L. F.; Pittenauer, E.; Allmaier, G.; Kirchner, K. *Organometallics* **2014**, *33*, 6905–6914. (d) Bichler, B.; Holzhacker, C.; Stöger, B.; Puchberger, M.; Veiros, L. F.; Kirchner, K. *Organometallics* **2013**, *32*, 4114–4121. (e) Benito-Garagorri, D.; Becker, E.; Wiedermann, J.; Lackner, W.; Pollak, M.; Mereiter, K.; Kisala, J.; Kirchner, K. *Organometallics* **2006**, *25*, 1900–1913. (f) Benito-Garagorri, D.; Wiedermann, J.; Pollak, M.; Mereiter, K.; Kirchner, K. *Organometallics* **2007**, *26*, 217–222. (g) Benito-Garagorri, D.; Puchberger, M.; Mereiter, K.; Kirchner, K. *Angew. Chem., Int. Ed.* **2008**, *47*, 9142–9145. (h) Gorgas, N.; Stöger, B.; Veiros, L. F.; Kirchner, K. *ACS Catal.* **2016**, *6*, 2664–2672.
- (17) Bertini, F.; Gorgas, N.; Stöger, B.; Peruzzini, M.; Veiros, L. F.; Kirchner, K.; Gonsalvi, L. *ACS Catal.* **2016**, *6*, 2889–2893.
- (18) Junge, H.; Boddien, A.; Capitta, F.; Loges, B.; Noyes, J. R.; Gladiali, S.; Beller, M. *Tetrahedron Lett.* **2009**, *50*, 1603–1606.
- (19) Langer, R.; Iron, M. A.; Konstantinovskii, L.; Diskin-Posner, Y.; Leitens, G.; Ben-David, Y.; Milstein, D. *Chem. - Eur. J.* **2012**, *18*, 7196–7209.
- (20) Gas mixture analyses were carried out by FTIR spectroscopic methods described in previous publications. For details see: (a) Morris, D. J.; Clarkson, G. J.; Wills, M. *Organometallics* **2009**, *28*, 4133–4140. (b) Guerriero, A.; Bricout, H.; Sordakis, K.; Peruzzini, M.; Monflier, E.; Hapiot, F.; Laurenczy, G.; Gonsalvi, L. *ACS Catal.* **2014**, *4*, 3002–3012.